R. & M. No. 2669
(12,023)
A.R.C. Technical Report

MINISTRY OF SUPPLY

AERONAUTICAL RESEARCH COUNCIL
REPORTS AND MEMORANDA

Conical Flow as a Result of Shock and Boundary-Layer Interaction on a Probe

By
J. LUKASIEWICZ

LONDON: HER MAJESTY'S STATIONERY OFFICE
1952
THREE SHILLINGS NET

Conical Flow as a Result of Shock and Boundary-Layer Interaction on a Probe

By

J. Lukasiewicz

Communicated by the Principal Director of Scientific Research (Air), Ministry of Supply

Reports and Memoranda No. 2669*

September, 1948

Summary.—The formation of a conical shock and a conical region of flow separation originating from the tip of a thin traversing tube was observed in a supersonic tunnel as a result of interaction of a strong shock with the boundary layer on the tube surface. The angles of the conical shock and separation surfaces and the static pressure in the separation region are in good agreement with the theoretical conical flow solutions.

The extent of the conical flow illustrated should act as a warning against the use of static pressure tubes for measuring pressures in the regions of strong shocks.

1. *Introduction.*—The interaction of shocks with the boundary-layer results, in general, in complex flows involving pressure and velocity discontinuities and separation regions. The classical boundary-layer theory is no longer valid in these cases and, so far, only experimental investigations of such phenomena are possible. The unsteadiness of flows of this type, the influence of subsonic downstream conditions and hysteresis effects often render the experimental investigations and generalization of the results difficult. It appears, however, that in certain cases the shock boundary-layer interaction leads to a simple conical flow, which can be compared with the exact inviscid solutions. This particular type of interaction phenomena will be described here.

2. *Symbols*—

M	Free stream Mach number
P	Free stream static pressure
P_c	Static pressure on cone surface, in conical flow
P_0	Stagnation pressure
P_0'	Pitot pressure
θ_c	Cone or conical separation vertex half-angle
θ_s	Conical shock vertex half-angle

3. *Earlier Investigations.*—It is now generally known that true static pressure readings cannot be obtained in shock regions, whether the pressure is measured by holes flush with the body or wall surface or by static-pressure tubes. This problem was perhaps first investigated by Ferri[1], who measured pressure downstream of a shock simultaneously by two static tubes of different length. The static-pressure readings were equal and agreed with theoretical values provided both tubes were situated downstream of the shock but a smaller pressure was indicated by the longer tube when it passed through the shock. Similarly, a higher pressure was indicated by the static tube upstream of the shock as compared with the pressure recorded by a static tube so constructed that its connection did not pass through the shock.

* R.A.E. Tech. Note Aero. 1968, received 29th December, 1948.

51886 A

Analogous discrepancies in magnitudes of flow velocity in shock regions, as determined from interference photographs of the flow and from the angle of Mach waves (measured from shadowgraphs) produced by thin, pointed wire probes, were reported by Ladenburg, Van Voortis and Winckler[2]. They found that the interaction with the wire probe of a normal standing shock obtained in an under-expanded jet issuing from a convergent nozzle caused the formation of a conical shock and a conical region of flow separation. The conical flow developed from the tip of the probe or, when it was moved upstream, from the wire surface, as shown diagrammatically in Fig. 1. These observations were subsequently checked with the exact conical flow theory by Winckler[3], who compared the observed shock angle with the theoretical value for the observed angle of conical separation and local Mach number, which was determined from interferometer photographs. The agreement was not very good for under-expanded jets, presumably because of large variations of velocity in the jet, but was remarkably close (to within $2 \cdot 6$ deg of shock angle) in case of a uniform jet obtained with a convergent-divergent nozzle, over a range of Mach numbers from $1 \cdot 70$ to $2 \cdot 20$.

4. *Observations in Supersonic Wind Tunnel.*—The development of conical flow as a result of shock boundary-layer interaction has often been observed in $5 \cdot 5 \times 5 \cdot 5$-in. Supersonic Wind tunnel at the Royal Aircraft Establishment. A flow of this type formed around the pitot-static traversing tube on starting or stopping the tunnel, when the main shock moved across the working section. This is shown in Fig. 2 at a free stream Mach number of about $1 \cdot 85$. The measured flow separation cone half-angle θ_c is equal to about 21 deg, which, at $M = 1 \cdot 85$, gives a conical shock half angle $\theta_s = 41 \cdot 7$ deg. This compares well with the measured value of $\theta_s = 42$ deg.

In the experiments of the above type it was not possible to obtain a stable shock system and therefore, with the long exposure schlieren equipment available ($0 \cdot 02$ sec exposure), accurate visual observations could not be made and static pressure in the conical separation region could not be measured. It was found, however, that when the nozzle was moved downstream from its normal position, towards the traverse gear and diffuser sections of the tunnel, a very stable conical flow type of shock boundary-layer interaction was obtained.

The tunnel arrangement and details of the pitot-static traversing tube are shown in Fig. 3. The flat constant-area working-section liners, usually mounted between the nozzle and traverse liners, were omitted and a $2 \cdot 48$-Mach number nozzle was fitted directly upstream of the traverse liners. The traversing gear consisted of a bridge spanning the tunnel and holding a combined pitot-static tube, which could be moved along the tunnel axis, from outside, by means of a rack and pinion.

The sequence of schlieren observations of flow, as the traversing tube was moved upstream and downstream in the tunnel nozzle, is shown in Fig. 4. The shock system which caused the formation of the conical flow can be seen originating from the nozzle walls. In these experiments atmospheric air was used and in all photographs a rather intense condensation shock appears near the nozzle throat. Its reflections are propagated downstream and are seen superimposed on the images of conical flow.

In Fig. 4, photographs obtained during two runs are included and position of the pitot tube head is indicated in terms of x, the distance from the nozzle geometrical throat. The traversing tube occasionally vibrated but in general remained steady; the two flow conditions are shown in Fig. 4 at $x = 4 \cdot 4$ in. (in the first column from the left).

The range of tube positions for which the conical-flow configuration was obtained varied with the tunnel back pressure, which was controlled by a valve located between the tunnel diffuser and the pumps. With the lowest back pressure attainable, the conical configuration had disappeared by the time the pitot-tube head reached $x = 4 \cdot 4$ in., but, when the valve was partially closed, it could be induced to remain up to $x = 2 \cdot 7 \sim 1 \cdot 8$ in. It is evident from Fig. 4 that at these tube positions the large blockage due to separation may have been responsible for the breakdown of the conical regime.

The stages of transition from conical to normal undisturbed flow are shown by the three photographs taken at $x = 2 \cdot 4$ and $1 \cdot 9$ in. In the transition range the flow was unsteady, the vertex of the conical separation oscillating along the traverse tube. When the tube was moved further towards the throat undisturbed flow was obtained; at $x = 0 \cdot 4$ in. a detached bow wave formed ahead of the pitot tube. When, from this point, the traverse tube was moved in the opposite direction, the conical regime did not appear until a value of $x = 4 \cdot 9$ to $5 \cdot 9$ in. was reached.

A large-scale photograph of the conical flow regime is shown in Fig. 5.

The above visual observations were supplemented by simultaneous pitot-static pressure readings taken throughout one run. They are shown in Fig. 6 in terms of pitot-stagnation (P_0'/P_0) and static/stagnation (P/P_0) pressure ratios. The static pressure measurements agree with the observed position of the condensation shock. The hysteresis effect illustrated in Fig. 4 is clearly indicated by the differences in the static pressure recorded during traverses in the upstream and down-stream directions. The points at which the static pressure readings start to diverge are in good agreement with the observed points of transition from conical to undisturbed flow (and *vice-versa*), which are marked in Fig. 6, but the static pressure variation is different at the two ends of the hysteresis loop. Whereas the transition from conical to undisturbed flow at (static orifices' position $x \simeq 4 \cdot 5$ in.) is marked by a sudden drop of static pressure, the static pressure increases more gradually during the transition from undisturbed to conical flow and starts to rise some distance before the point of transition at $x \simeq 7 \cdot 45$ in. This is presumably due to the proximity of static holes at large x values, to the main tunnel shock.

The pitot pressure readings, as is evident from traverses in the two directions, are not affected by the formation of conical flow.

5. *Comparison with Conical Flow Theory.*—In order to compare visual and pressure observations with the conical flow theory, it was necessary to determine the Mach number distribution in the nozzle. Some difficulties were experienced due to the presence of the humidity shock and the influence of the main tunnel shock on static pressure readings. The Mach number, as determined from the ratios of pitot/stagnation, static/stagnation and pitot/static pressure is plotted in Fig. 7 over a range of x covering the formation of the conical flow regime. The effect of the condensation shock is to decrease the stagnation pressure and therefore, the Mach number based on P_0^1/P_0 and P/P_0, where P_0 is the stagnation pressure measured upstream of the condensation shock, would be expected to exceed the true value. Assuming that the presence of condensate does not affect the pitot-tube reading, a more accurate estimate of the Mach number is obtained from the local pitot/static pressure ratio: the Mach number so calculated is, in fact, lower than that based on either of the other two ratios. It increases from a value of $2 \cdot 1$ at $x = 3$ in. and remains substantially constant and equal to $2 \cdot 3$ for $x = 4 \cdot 7$ to $5 \cdot 8$ in. At larger values of x the validity of static pressure readings is doubtful; pitot pressure indicates a slight decrease in the Mach number. This estimate of Mach number distribution is in agreement with the results of other traverses made with the nozzle in the normal position and when atmospheric air was used. In one instance, the Mach number could be directly determined from the angle of wavelets originating from the pitot tube tip (Fig. 4, photograph for $x = 4 \cdot 4$ in.) and was found to be $2 \cdot 241$, which is in general agreement with Fig. 7.

The observed values of shock half-angle θ_s, cone half-angle θ_c and the ratio of the static pressures for the two regimes are plotted in Fig. 8, in which also curves for conical flow at a constant free-stream Mach number $M = 2$ and $2 \cdot 5$ are shown. The position of pitot-tube head corresponding to the experimental points is marked in terms of x in.

The observed angles θ_s and θ_c correspond to conical flow at a Mach number from about $2 \cdot 2$ to $2 \cdot 4$ which is in agreement with the distribution shown in Fig. 7. Pitot position at small values of x corresponds to a lower Mach number.

The ratios of static pressures, which were considered reliable in the range of x from $4 \cdot 7$ to $5 \cdot 7$ in., Fig. 6, are plotted in Fig. 8 in terms of simultaneously observed separation and shock angles. Curves of the ratio of static pressure on the cone surface P_c to the free stream static pressure P in conical flow at $M = 2$ and $2 \cdot 5$ are shown for comparison. The agreement is again good, the experimental points indicating a Mach number of $2 \cdot 3$ or smaller, as would be expected for the corresponding pitot tube positions.

Similar traverses to those described above were made with the pitot-static tube fitted with a sleeve, as shown in Fig. 3. The resulting change in the boundary layer flow over the traversing tube had no noticeable influence on the development of conical separation and limits of the hysteresis loop. The conical flow obtained is shown in Fig. 9 for pitot-tube position $x = 3 \cdot 4$ in. The angles $\theta_s = 36$ deg and $\theta_c = 21$ deg agree with those measured previously in the same pitot tube position, Fig. 8.

6. *Conclusions.*—The tunnel observations here analysed and earlier American investigations have shown that in certain cases interaction of strong, substantially normal shocks with the boundary layer formed on cylindrical bodies, such as small diameter wires or tubes, results in the formation of a conical shock and a conical region of flow separation, originating from the tip of the body or from its surface and, in some cases, extending throughout the supersonic stream. The observed angles of the conical shock corresponding to the angles of the separation surfaces agree with the theoretical conical flow solutions. The static pressure measured on the axis of the conical separation region, some distance from its vertex, is equal, to a good approximation, to the theoretical pressure obtained on the cone surface, for the observed shock and separation angle.

In common with other types of supersonic flows involving shocks, the formation of conical separation exhibits hysteresis characteristics.

From the point of view of experimental technique, the phenomenon of conical separation of flow is significant in that it accounts for the failure of direct pressure measurement by means of a static tube in the regions near strong shocks. In the present tests the error in the static pressure thus estimated upstream of a shock could amount to 100 per cent. For weak shocks, the interaction effects are smaller and static tube traverses of weak shocks appear to give reliable results[5]. From several tests of central body type supersonic inlets and observations of shock and boundary layer interaction on flat walls[4] it appears that separation is not appreciable when the static pressure ratio across the shock is smaller than $1 \cdot 8$, corresponding to a normal shock at $M = 1 \cdot 3$.

REFERENCES

No.	*Author*	*Title, etc.*
1	A. Ferri	Experiments at Supersonic Speed on a Biplane of the Busemann type. Atti di Guidonia No. 37–38, 1940. A.R.C. Report No. 5921. (Unpublished.)
2	R. Ladenburg, C. C. Van Voortis and J. Winckler	Interferometric Study of Supersonic Phenomena (Part I). Princeton University, Navord Report 69–46 April, 1946.
3	J. Winckler	Interferometric Study of Supersonic Phenomena (Part III). Princeton University, Navord Report 7–47 February, 1947.
4	A. Fage and R. F. Sargent ..	Shock Wave and Boundary Layer Phenomena near a Flat Surface. *Proc. Roy. Soc.* A, 190, 1947, 1–20. A.R.C. Report No. 8964.
5	J. Ackeret, F. Feldmann and N. Rott	Investigations on Compression Shocks and Boundary Layers in Fast Moving Gases. E.T.H. Report No. 10, Zurich. 1946. A.R.C. Report No. 10,044. (Unpublished.)

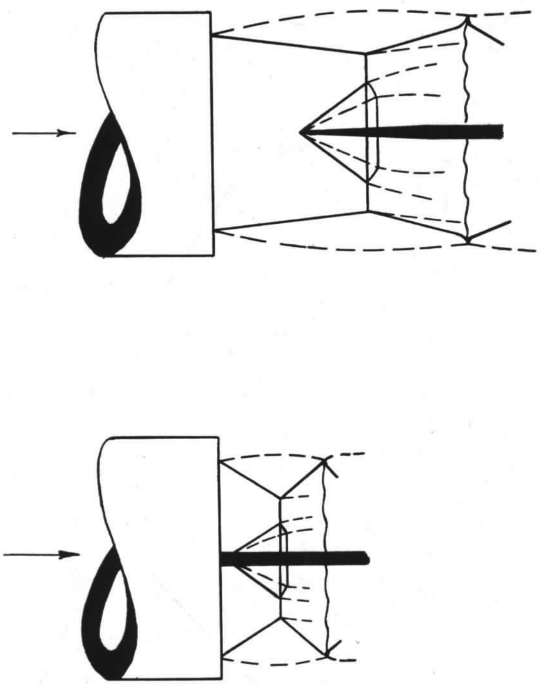

FIG. 1. Conical flow around a wire probe as observed by Winckler (Ref. 3) in a free jet.

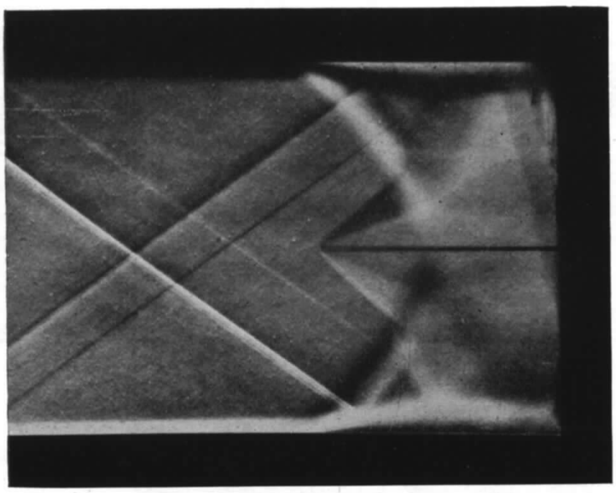

FIG. 2. Formation of conical flow on traversing tube at $M = 1 \cdot 85$

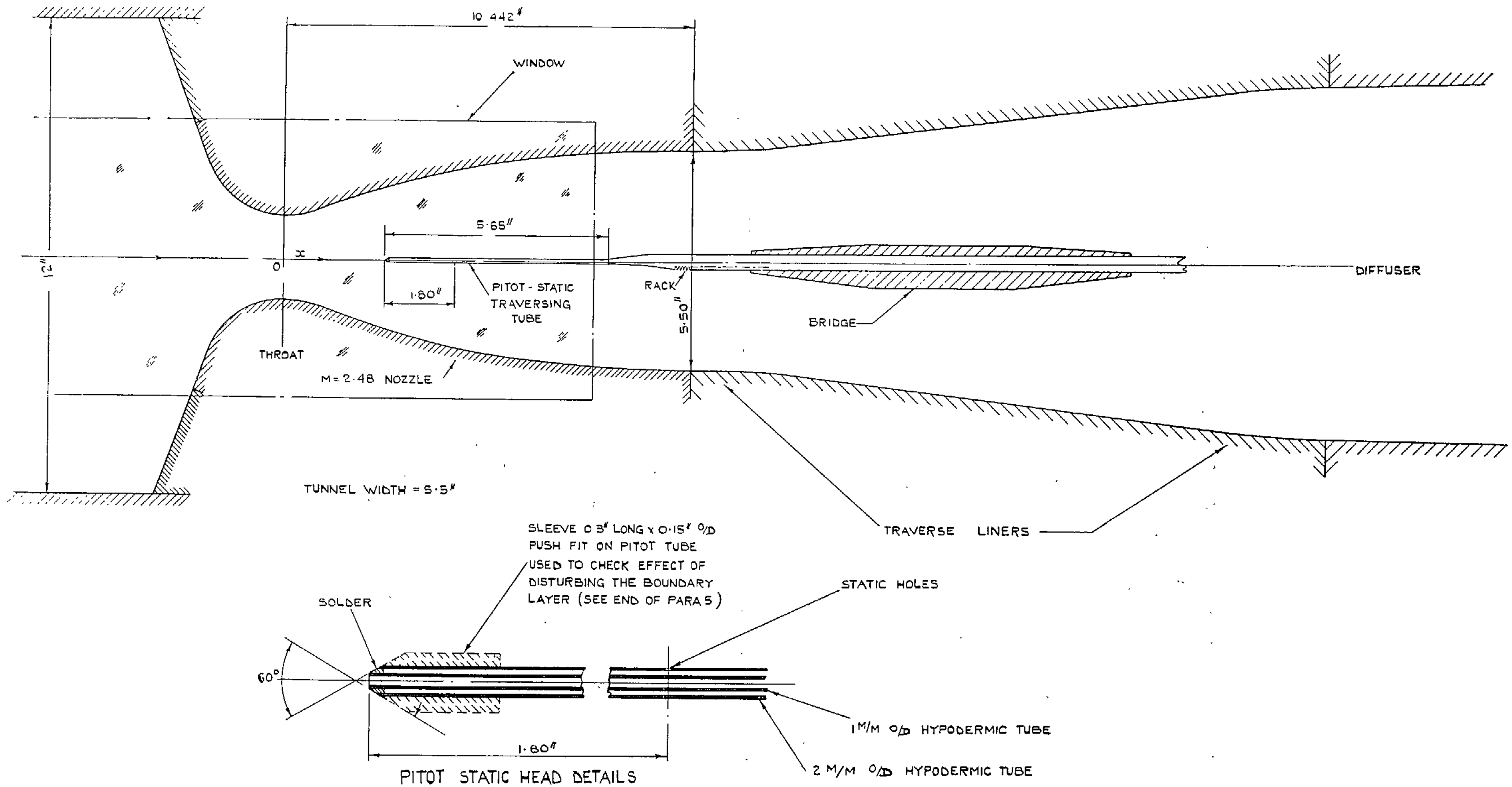

FIG. 3. Tunnel arrangement and details of pitot-static traversing tube.

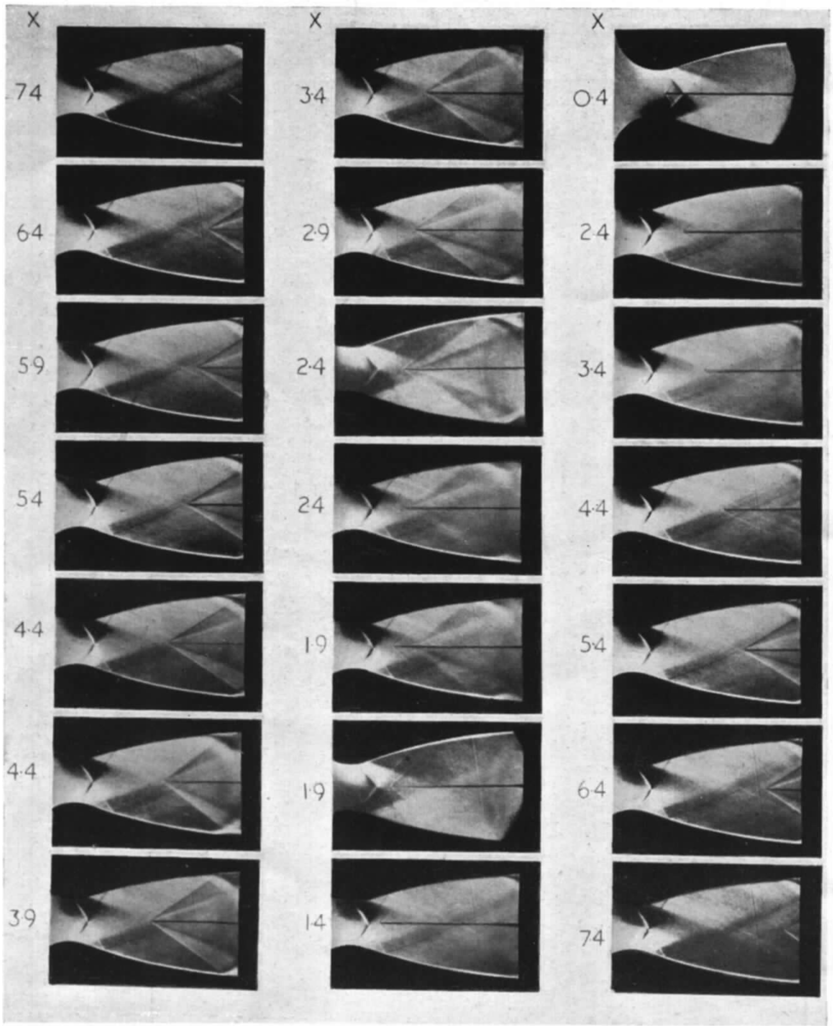

X = Distance from nozzle geometrical throat to pitot tube, inches

FIG. 4. Formation of conical flow on pitot-static traversing tube.

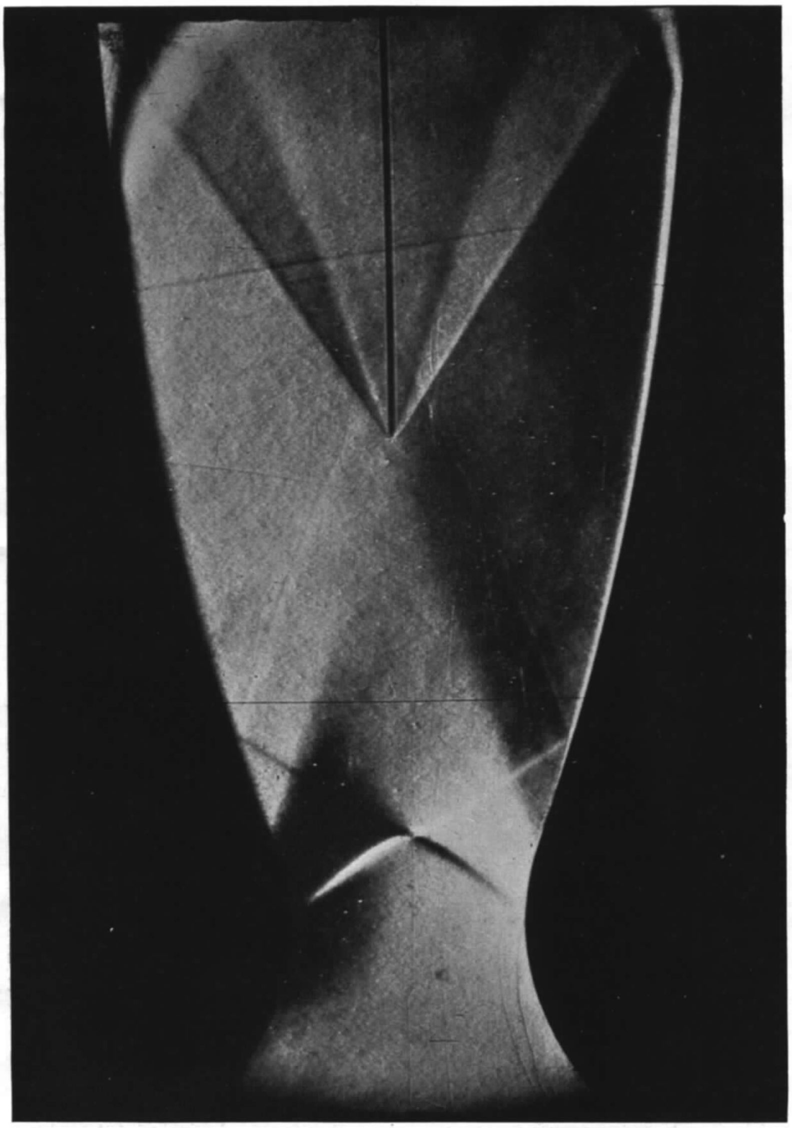

FIG. 5. Conical separation of flow (pitot tube head at $x = 4{\cdot}4$ in.).

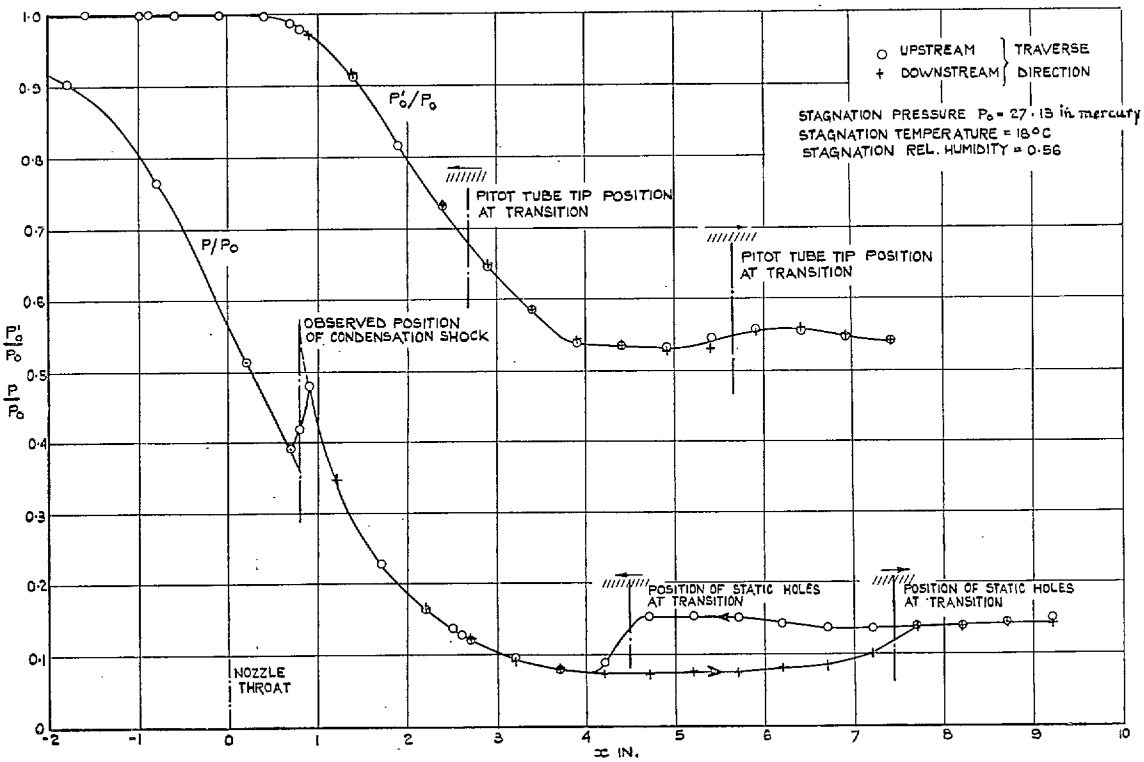

FIG. 6. Pitot-static pressure traverse.

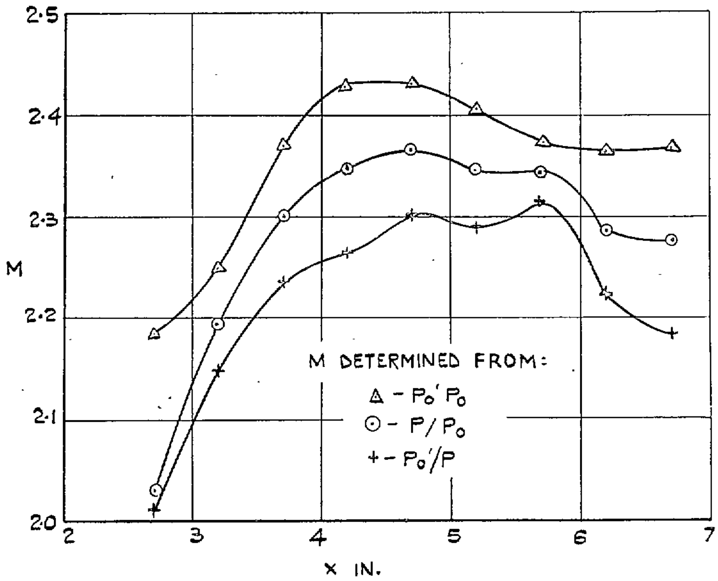

FIG. 7. Mach number distribution.

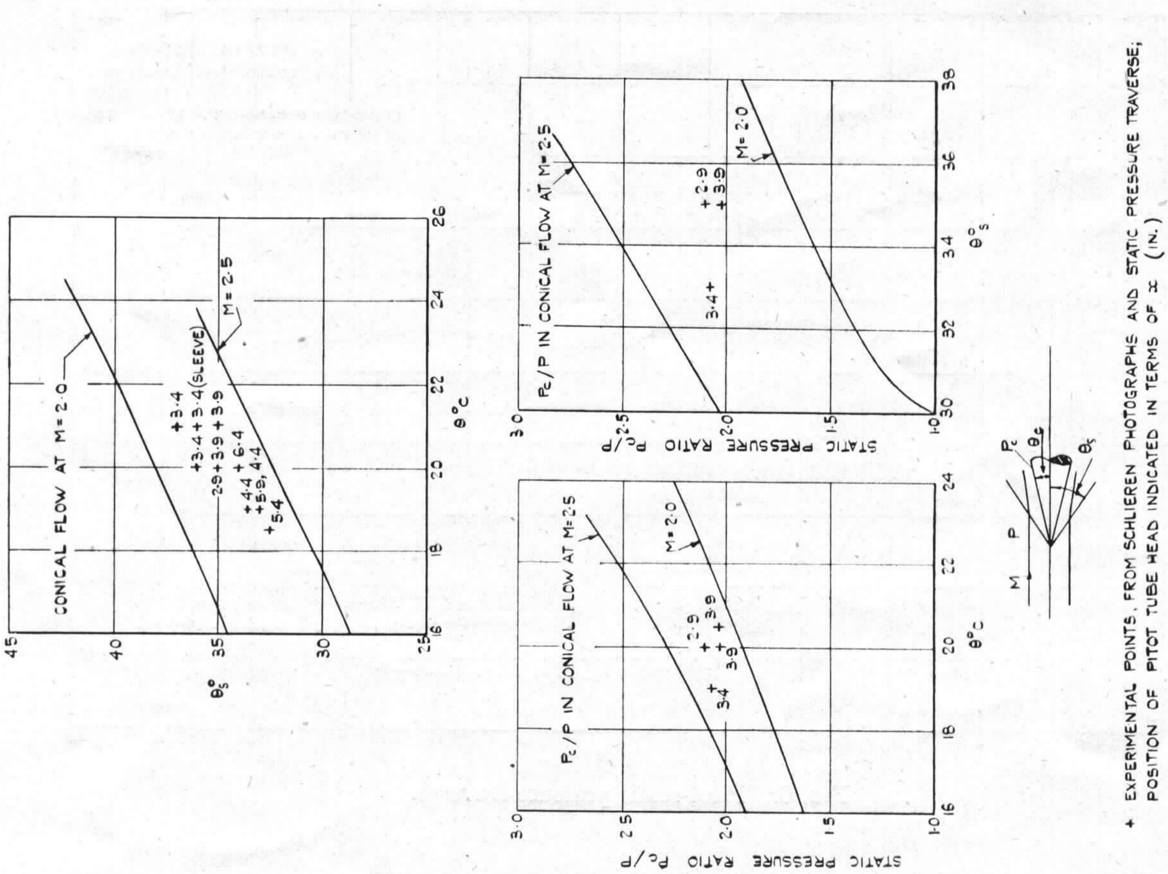

FIG. 8. Comparison of observed values of conical separation angle (θ_c), shock angle (θ_s) and static pressure ratio with conical flow theory.

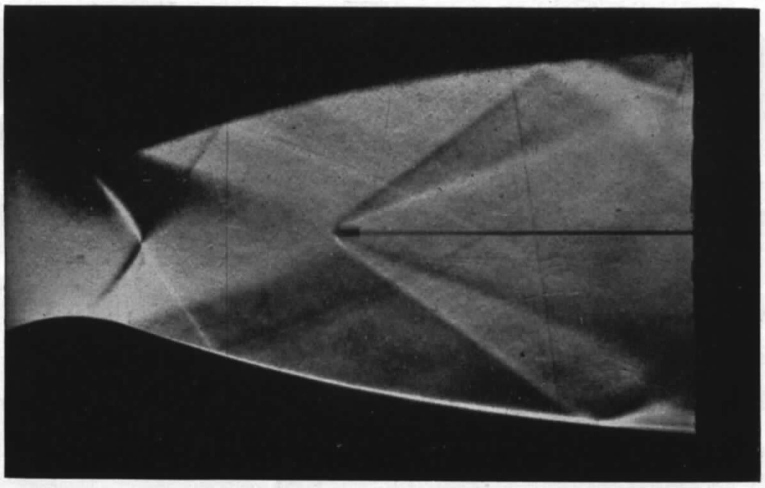

FIG. 9. Conical flow formed on traversing tube fitted with cylindrical sleeve ($x = 3{\cdot}4$ in.).

(51886) Wt. 15/680 K.5 7/52 Hw.

PRINTED IN GREAT BRITAIN

R. & M. No. 2669
(12,023)
A.R.C. Technical Report

Publications of the Aeronautical Research Council

ANNUAL TECHNICAL REPORTS OF THE AERONAUTICAL RESEARCH COUNCIL (BOUND VOLUMES)—

1934–35 Vol. I. Aerodynamics. *Out of print.*
Vol. II. Seaplanes, Structures, Engines, Materials, etc. 40*s.* (40*s.* 8*d.*)

1935–36 Vol. I. Aerodynamics. 30*s.* (30*s.* 7*d.*)
Vol. II. Structures, Flutter, Engines, Seaplanes, etc. 30*s.* (30*s.* 7*d.*)

1936 Vol. I. Aerodynamics General, Performance, Airscrews, Flutter and Spinning. 40*s.* (40*s.* 9*d.*)
Vol. II. Stability and Control, Structures, Seaplanes, Engines, etc. 50*s.* (50*s.* 10*d.*)

1937 Vol. I. Aerodynamics General, Performance, Airscrews, Flutter and Spinning. 40*s.* (40*s.* 10*d.*)
Vol. II. Stability and Control, Structures, Seaplanes, Engines, etc. 60*s.* (61*s.*)

1938 Vol. I. Aerodynamics General, Performance, Airscrews. 50*s.* (51*s.*)
Vol. II. Stability and Control, Flutter, Structures, Seaplanes, Wind Tunnels, Materials. 30*s.* (30*s.* 9*d.*)

1939 Vol. I. Aerodynamics General, Performance, Airscrews, Engines. 50*s.* (50*s.* 11*d.*)
Vol. II. Stability and Control, Flutter and Vibration, Instruments, Structures, Seaplanes, etc. 63*s.* (64*s.* 2*d.*)

1940 Aero and Hydrodynamics, Aerofoils, Airscrews, Engines, Flutter, Icing, Stability and Control, Structures, and a miscellaneous section. 50*s.* (51*s.*)

Certain other reports proper to the 1940 volume will subsequently be included in a separate volume.

ANNUAL REPORTS OF THE AERONAUTICAL RESEARCH COUNCIL—

1933–34	1*s.* 6*d.* (1*s.* 8*d.*)
1934–35	1*s.* 6*d.* (1*s.* 8*d.*)
April 1, 1935 to December 31, 1936.	4*s.* (4*s.* 4*d.*)
1937	2*s.* (2*s.* 2*d.*)
1938	1*s.* 6*d.* (1*s.* 8*d.*)
1939–48	3*s.* (3*s.* 2*d.*)

INDEX TO ALL REPORTS AND MEMORANDA PUBLISHED IN THE ANNUAL TECHNICAL REPORTS, AND SEPARATELY—

April, 1950 R. & M. No. 2600. 2*s.* 6*d.* (2*s.* 7½*d.*)

INDEXES TO THE TECHNICAL REPORTS OF THE AERONAUTICAL RESEARCH COUNCIL—

December 1, 1936 — June 30, 1939.	R. & M. No. 1850.	1*s.* 3*d.* (1*s.* 4½*d.*)
July 1, 1939 — June 30, 1945.	R. & M. No. 1950.	1*s.* (1*s.* 1½*d.*)
July 1, 1945 — June 30, 1946.	R. & M. No. 2050.	1*s.* (1*s.* 1½*d.*)
July 1, 1946 — December 31, 1946.	R. & M. No. 2150.	1*s.* 3*d.* (1*s.* 4½*d.*)
January 1, 1947 — June 30, 1947.	R. & M. No. 2250.	1*s.* 3*d.* (1*s.* 4½*d.*)

Prices in brackets include postage.

Obtainable from

HER MAJESTY'S STATIONERY OFFICE

York House, Kingsway, LONDON, W.C.2 423 Oxford Street, LONDON, W.1
P.O. Box 569, LONDON, S.E.1
13a Castle Street, EDINBURGH, 2 1 St. Andrew's Crescent, CARDIFF
39 King Street, MANCHESTER, 2 Tower Lane, BRISTOL, 1
2 Edmund Street, BIRMINGHAM, 3 80 Chichester Street, BELFAST

or through any bookseller.

S.O. Code No. 23-2669